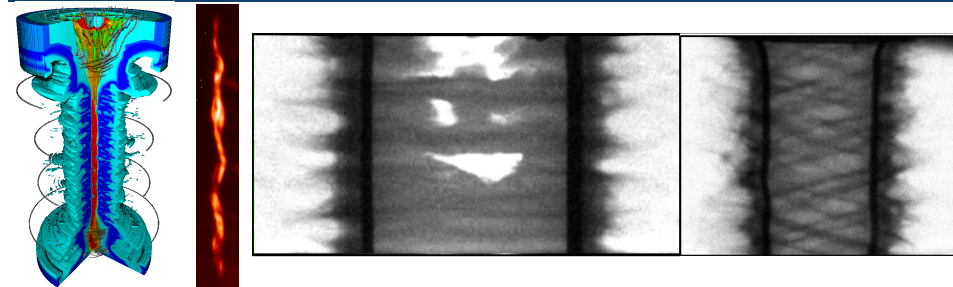
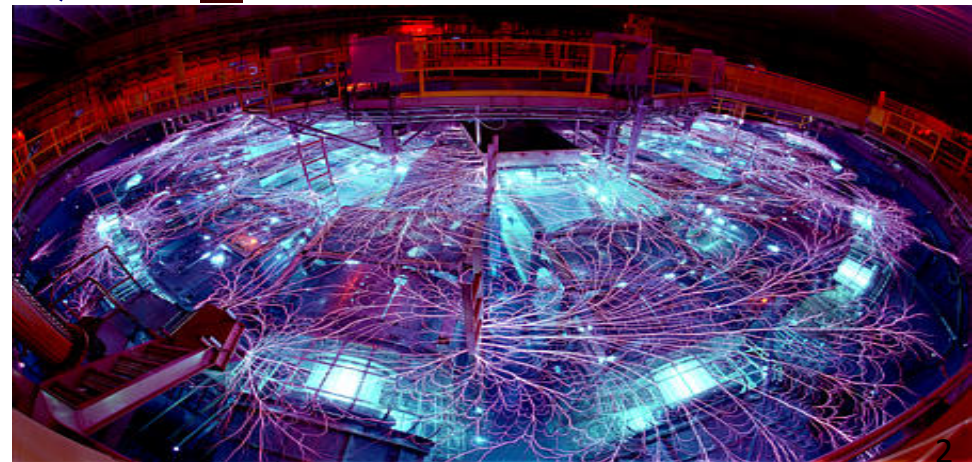


Diagnosing fuel magnetization with secondary neutrons

*Exceptional service
in the national interest*



Paul Schmit
October 6th, 2015



Sandia National Laboratories is a multi-program laboratory managed and operated by Sandia Corporation, a wholly owned subsidiary of Lockheed Martin Corporation, for the U.S. Department of Energy's National Nuclear Security Administration under contract DE-AC04-94AL85000.

This talk was made possible by the dedicated work of many...

Patrick Knapp¹, Stephanie Hansen¹, Kelly Hahn¹, Matt Gomez¹, Ryan McBride¹, Dean Rovang¹, Gordon Chandler¹, Eric Harding¹, Chris Jennings¹, Steve Slutz¹, Adam Sefkow¹, Dan Sinars¹, Kyle Peterson¹, Mike Cuneo¹, Tom Awe¹, Matt Martin¹, Carlos Ruiz¹, Gary Cooper¹, Bill Stygar¹, Mark Savage¹, Mark Herrmann³, Gregory Rochau¹, John Porter¹, Ian Smith¹, Matthias Geissel¹, Brent Blue³, Kurt Tomlinson², Diana Schroen², Robert Stamm⁴, Ray Leeper⁵, Charlie Nakhleh⁵

... And many many more

¹*Sandia National Laboratories, Albuquerque, NM*

²*General Atomics, San Diego, CA*

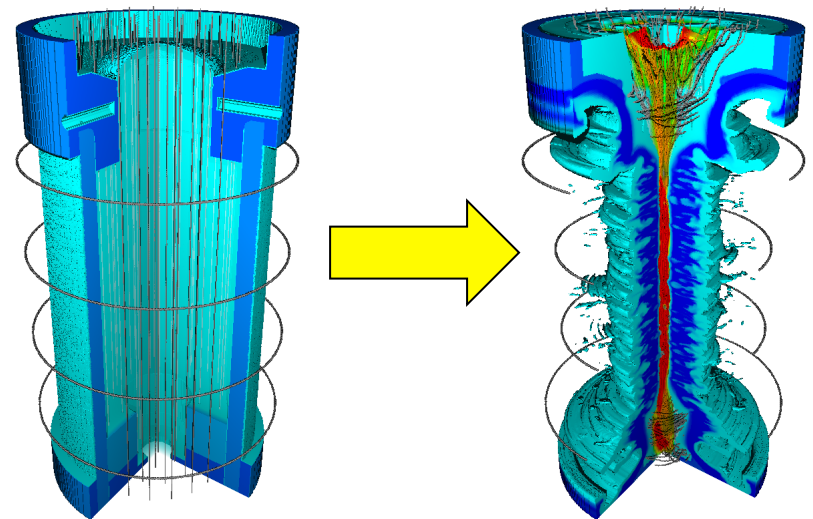
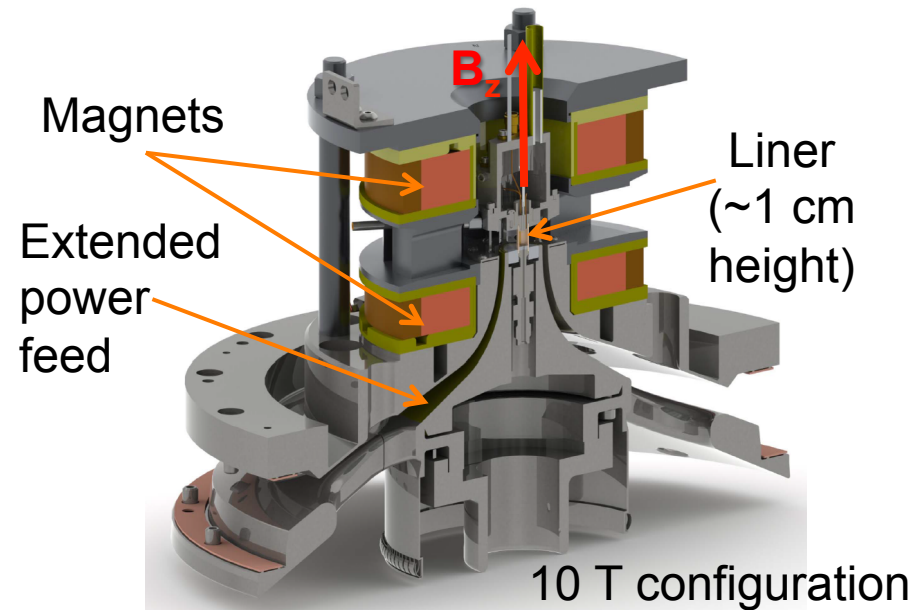
³*Lawrence Livermore National Laboratory, Livermore, CA*

⁴*Raytheon Ktech, Albuquerque, NM*

⁵*Los Alamos National Laboratory, Los Alamos, NM*

Purpose of pre-imposed B_z field in MagLIF

- $O(10\text{ T})$ B_z field applied to entire liner/fuel region prior to implosion
- Throughout implosion, B_z amplified by flux compression
- Thermal transport (primarily by electrons) to cold walls inhibited by B_z field
- B_z field also traps burn products at stagnation, necessary for ignition



Compressing the seed magnetic field is crucial, but losses can occur

Two major flux loss mechanisms

- Resistive diffusion
 - Reasonably well understood
 - Depends primarily on material EOS
- Nernst Thermoelectric effect
 - Driven by thermal gradients
 - Acts to transport field from hot core plasma to cold edge plasma/liner
 - Loss rate depends strongly on preheat energy and initial field strength (hall parameter and temp. gradient)
 - Not present in all integrated models

Approximate Global Nernst Loss Term

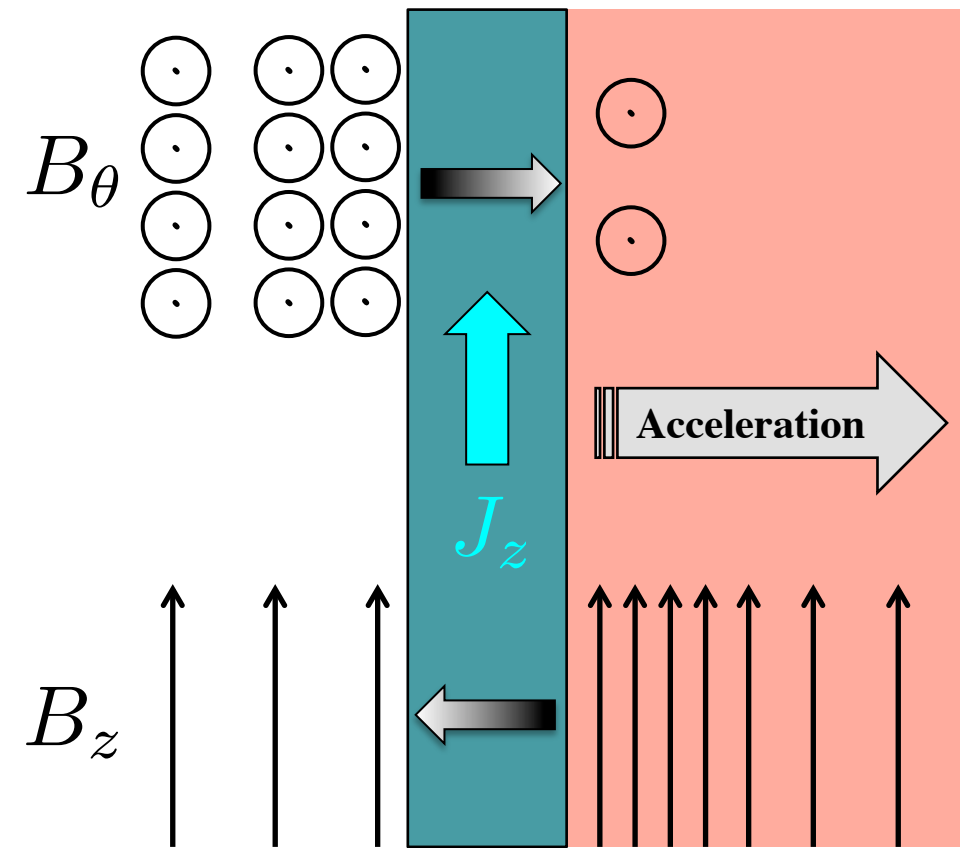
$$\dot{\Phi}_{zg} = -2\pi r \mathcal{F}(x_e) \nabla T$$

$$\mathcal{F}(x_e) = \frac{1.5x_e^3 + 3.053x_e}{x_e^4 + 14.79x_e^2 + 3.7703}$$

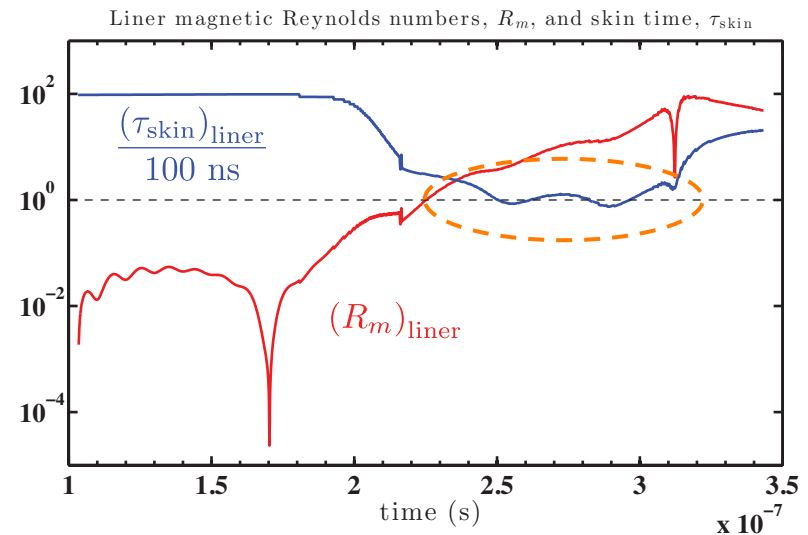
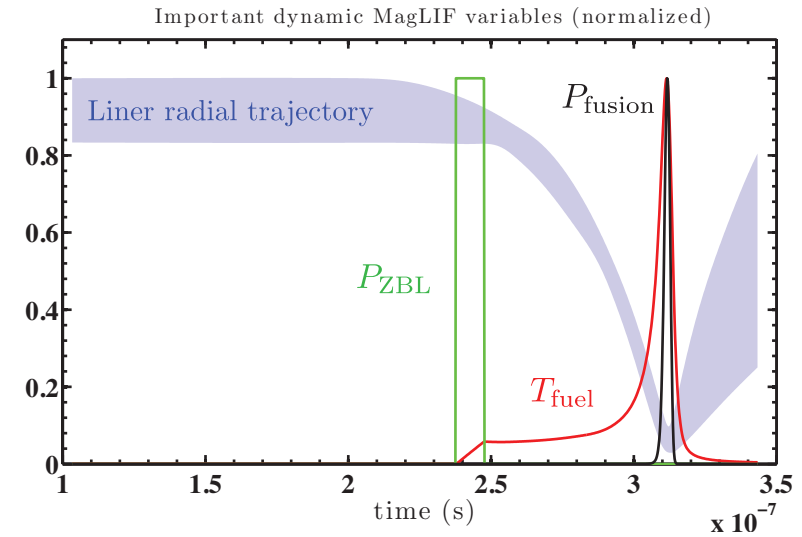
$$x_e = \omega_{ce} \tau_{ei}$$

$$\dot{\Phi}_{zg} \propto \frac{\nabla T}{x_e} \text{ when } x_e \gg 1$$

MagLIF magnetic environment: the liner



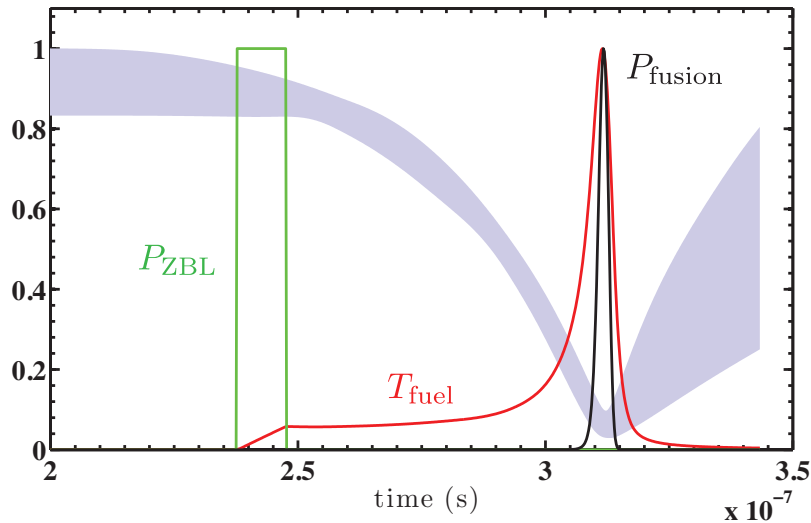
Liner can compress flux effectively, but some drive B_θ diffuses in through liner, and some B_z leaks out through liner



MagLIF magnetic environment: the fuel

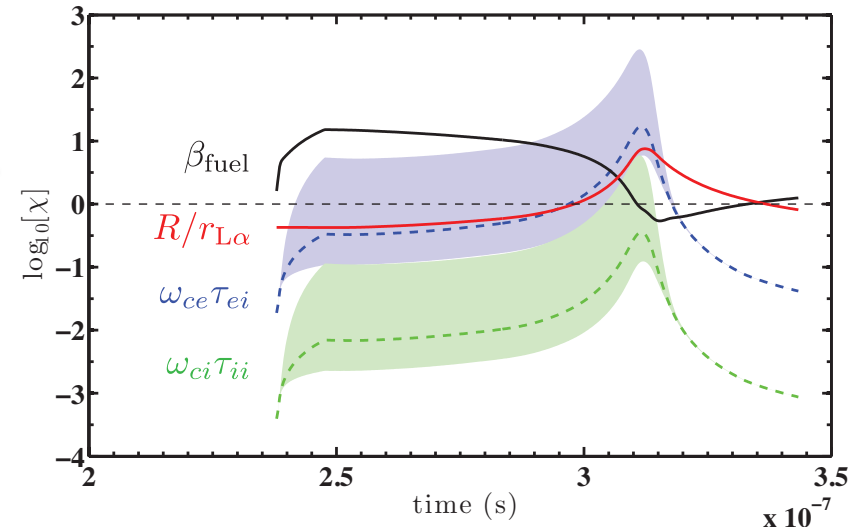
- Hottest e^- magnetized after preheat, all e^- magnetized by stagnation
- Most fuel ions aren't magnetized
- Fusion α 's confined at stagnation
- $\beta \gg 1$ for *most* of implosion

Important dynamic MagLIF variables (normalized)

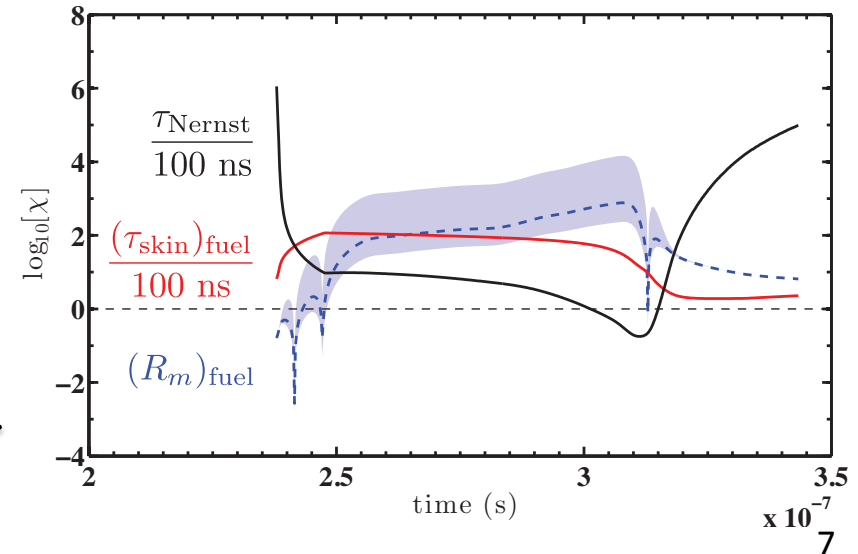


- Magnetic flux losses from fuel not predicted to be catastrophic
- Nernst losses *can* exceed diffusive losses

Confinement-related fuel quantities

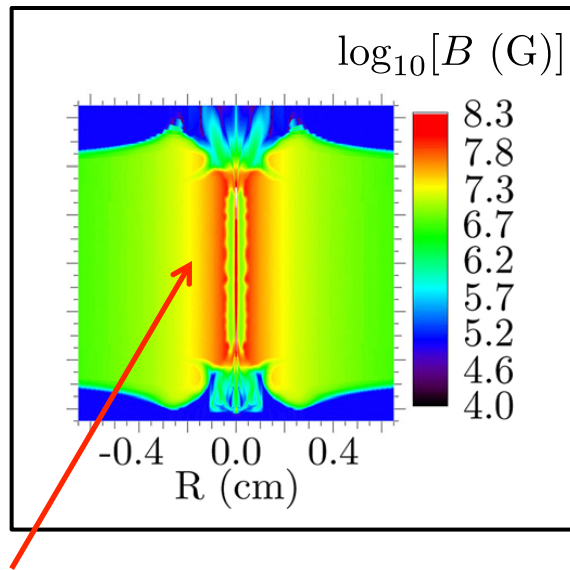


Flux-loss-related fuel quantities

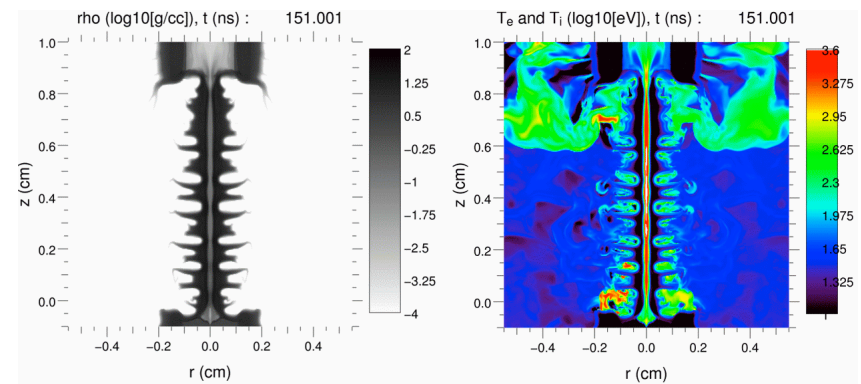
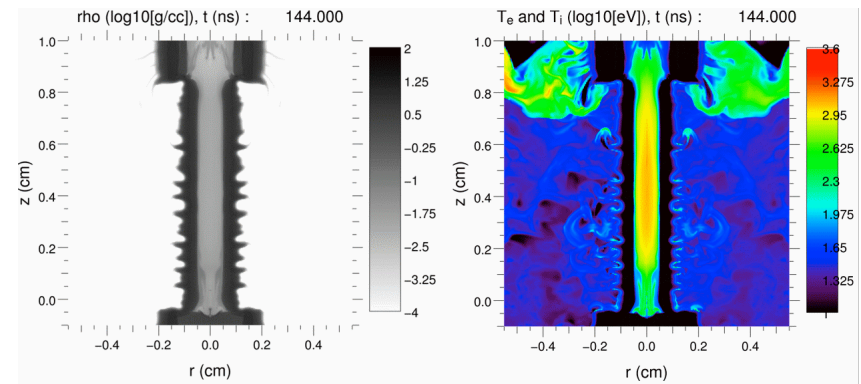
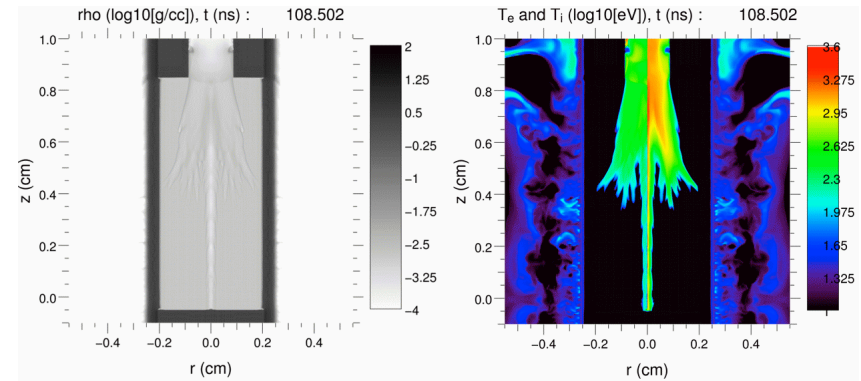


Integrated simulation predictions for B-field

- Integrated simulations use rad-MHD codes HYDRA and LASNEX
- W/o Nernst effects, $\Phi_{\text{loss}} \sim 26\text{-}47\%$ in near-term experiments*, with final $B_z \sim 50\text{-}100$ MG, $R/r_\alpha \sim 1.6\text{-}2.9$
- With Nernst effects, Φ_{loss} is greater**, but abates with higher initial B_z

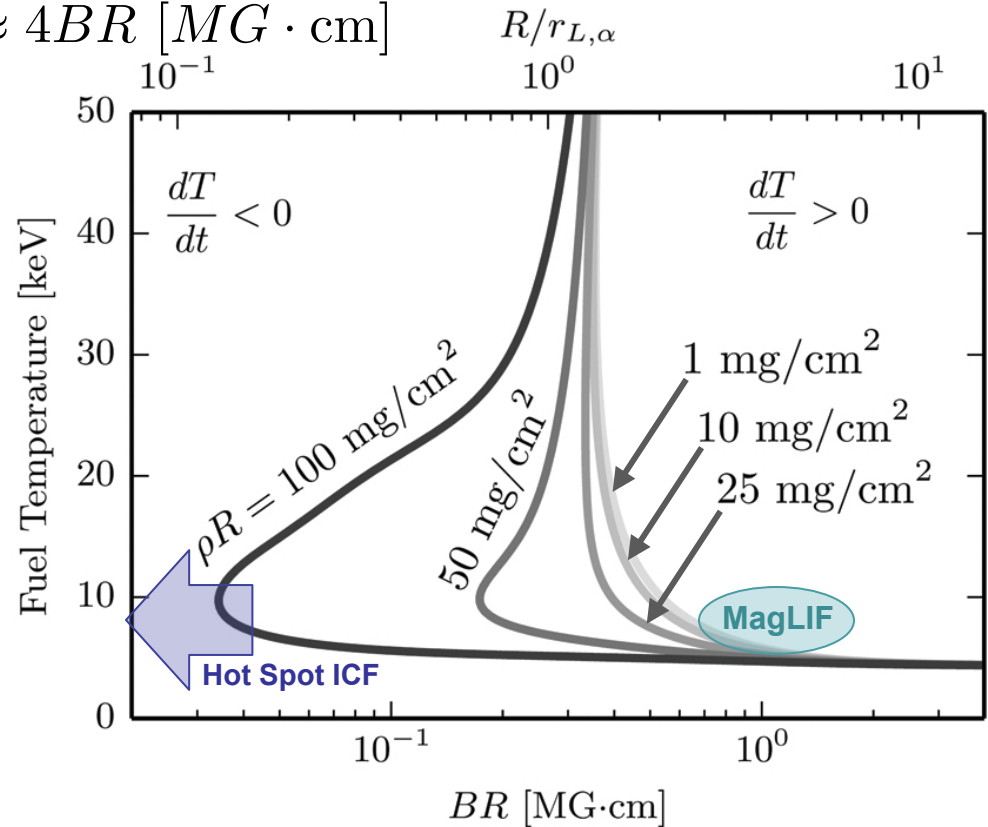
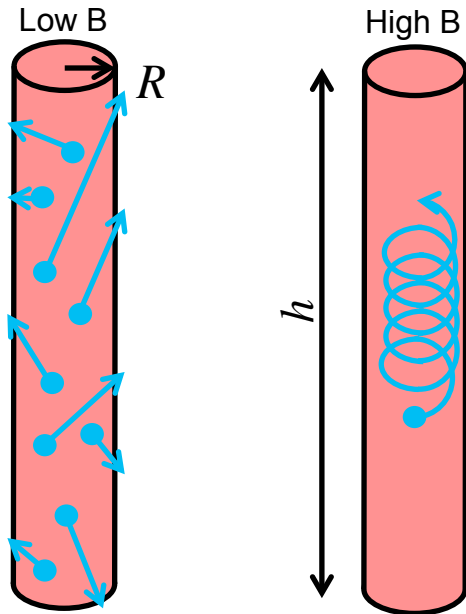


Note significant volume of high drive B_θ surrounds stagnated column of compressed B_z



BR supplements ρR as a fundamental confinement parameter for MIF plasmas

$$\frac{R}{r_\alpha} = \frac{BR [T \cdot \text{cm}]}{26.5} = \frac{BR [G \cdot \text{cm}]}{2.65e5} \approx 4BR [MG \cdot \text{cm}]$$



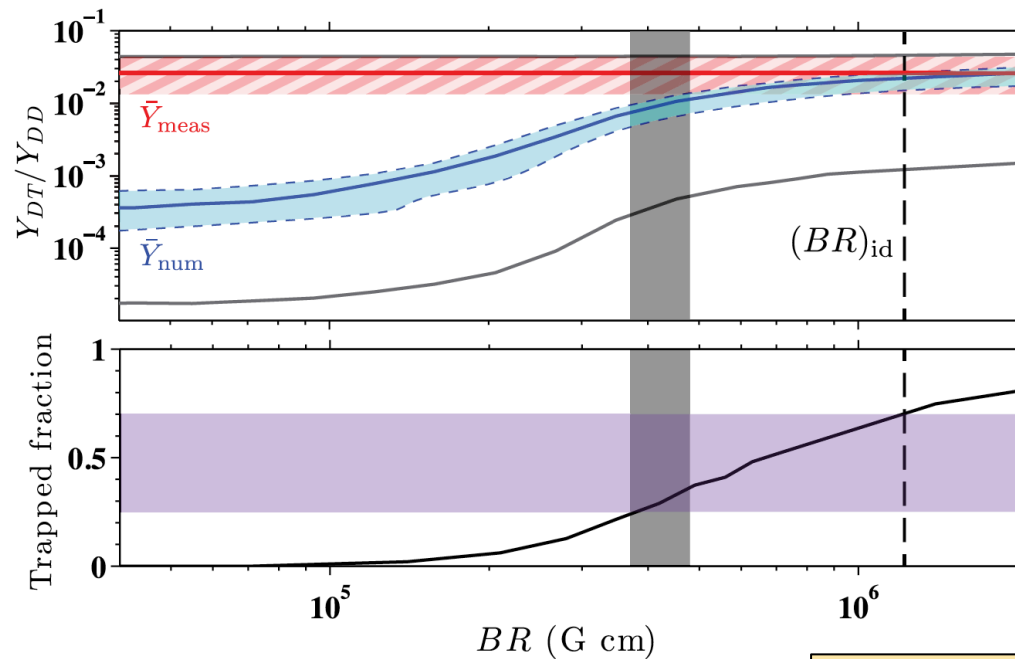
Magnetizing the fuel accomplishes two things

- Limits conduction losses from the electrons during implosion and stagnation
- Traps alpha particles allowing them to deposit their energy at much lower fuel ρR than otherwise possible

Fraction of trapped α 's (tritons) is a function of **BR** only*

In situ probing techniques will not allow us to diagnose flux compression and its effects in integrated experiments, new techniques required

Magnetic field confines and alters paths of DD tritons, encoding a signature of B-field during burn in the secondary neutron emission



Detailed analysis of Secondary DT neutrons and stagnation conditions gives:

- Stagnation $BR \sim 4 \times 10^5$ $G \cdot cm$, 14-17x initial BR
- Many charged reaction products are *magnetized* and confined at stagnation!
- First experimental confirmation in an HED experiment!

P.F. Schmit, P.F. Knapp *et al.* Phys. Rev. Lett. **113**, 155004 (2014)

P.F. Knapp, P.F. Schmit *et al.* Phys. Plasmas **22**, 056312 (2015)

The data...

Updated Summary of Neutron-producing Roosevelt (MagLIF) Shots

July 13, 2015

K. Hahn, G. Chandler, C. Ruiz, G. Cooper, B. Jones, and J. Torres

	Shot 2591	Shot 2613	Shot 2584	Shot 2707	Shot 2708	Shot 2758	Shot 2769
Avg. DD Yield	2.0e12 +/- 25%	1.1e12 +/- 25%	5.3e11 +/- 25%	2.8e11 +/- 25%	1.8e11 +/- 25%	3.1e11 +/- 25%	1.1e11 +/- 25%
DT Yield	5.4e10 +/- 50%	1.2e10 +/- 25%	1.2e10 +/- 50%	4.5e9 +/- 25%	2.5e9 +/- 25%	3.9e9 +/- 25%	1.0e9 +/- 25%
DT/DD	2.7%	1.1%	2.3%	1.6%	1.4%	1.3%	0.9%
T_{bang} <small>(Lin reg, sent 10-13-14)</small>	3095.97 ns +/- 0.91 ns	3098.36 ns +/- 0.84 ns	3102.95 ns +/- 0.97 ns	3099.77 ns +/- 1.07 ns	3094.46 ns +/- 0.93 ns		
Avg. T_{ion}	2.5 keV +/- 30%	2.4 keV +/- 30%	2.0 keV +/- 30%	1.6 keV +/- 30%	1.1 keV +/- 30%	1.8 keV +/- 30%	1.1 keV +/- 30%

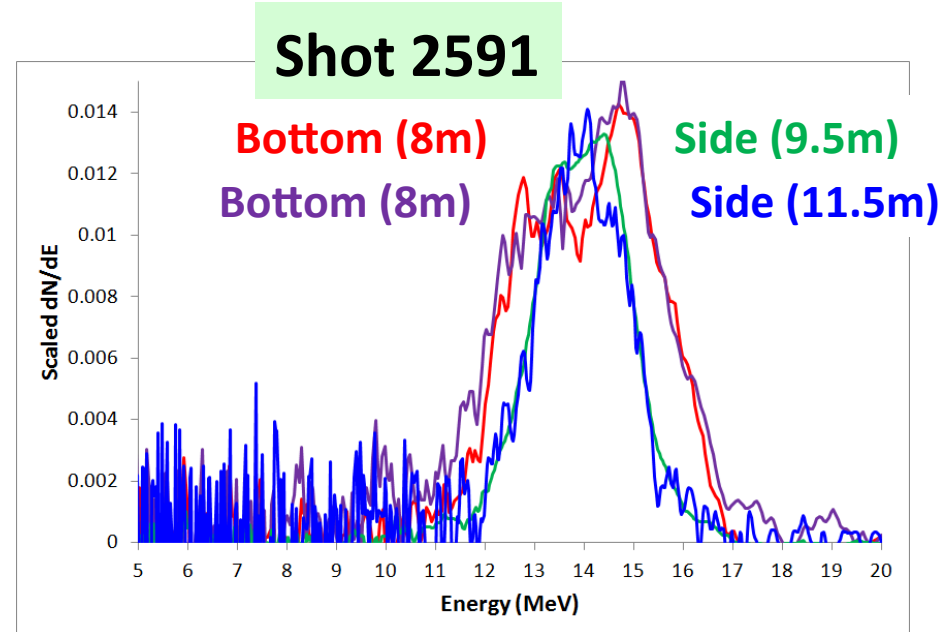
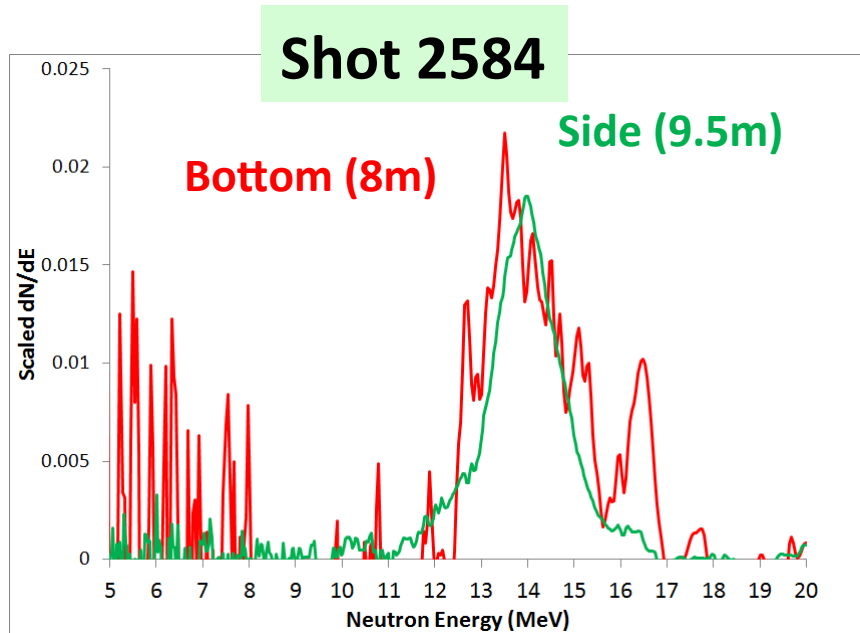
Sent to Paul Schmit: 7-16-15

Folder: Z:\DATA\ZR\1677\MagLIF\Presentations\Summary_Yields_Tions_7-13-15\sent_to_Paul_7-16-15

DT Spectral Differences Axial vs. Radial

Axial (bottom) spectra appear wider than radial spectra. Most notable for 2591.

K. Hahn, G. Chandler, C. Ruiz, G. Cooper, B. Jones, and J. Torres



- Note, amplitudes are arbitrary.
- Bottom signals at 8 m for 2584 were somewhat noisy, making it more difficult to distinguish axial/radial DT spectral differences.
- Originally used 7-m signal (better SNR) to show difference in axial/radial DT, but signal is distorted by Brems reflected signal.

- Note, amplitudes are arbitrary.
- Better signals for 2591 at 8m (and other locations) enable us to distinguish axial/radial DT spectral differences which are notable.
- *Working on background-subtracting 7-m signal (which should corroborate what above plot indicates).*

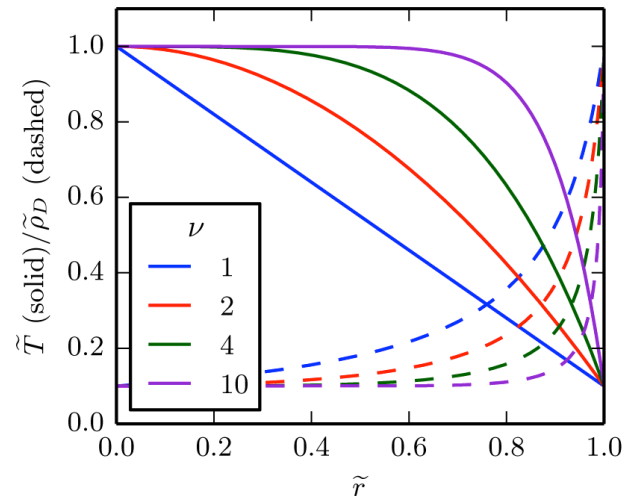
Secondary triton reactions modeled using a kinetic LFP model and MC reaction kinetics

Fast Ion Kinetic Model^[1-3]

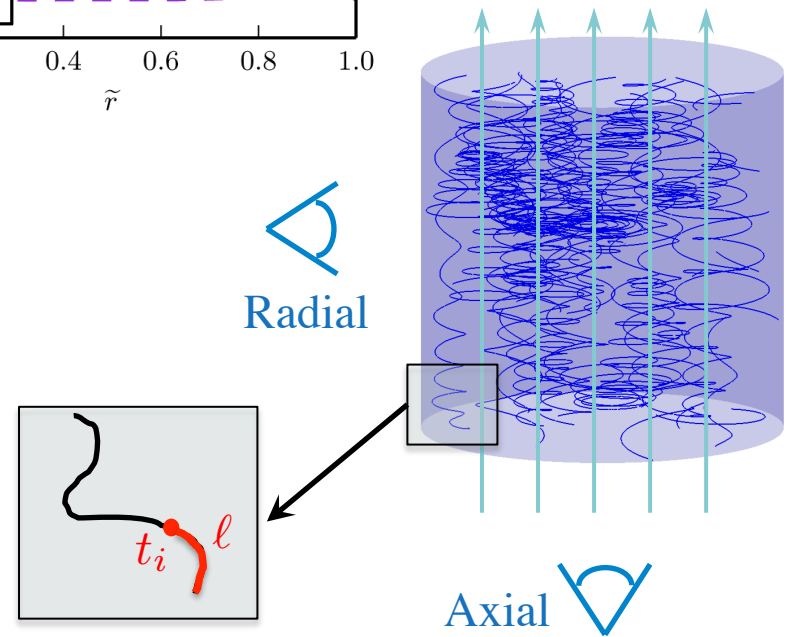
- Landau-Fokker-Planck model, electron-ion **AND** ion-ion collisions captured
- 1D prescribed isobaric fuel profiles w/ non-uniform B
- No B_ϕ or axial variations
- No time variations in fuel profile

MonteBurns^[1,2,4] Reaction Modeling

- Calculates neutron spectra and reaction probability for each triton quasi-particle from multiple viewing angles

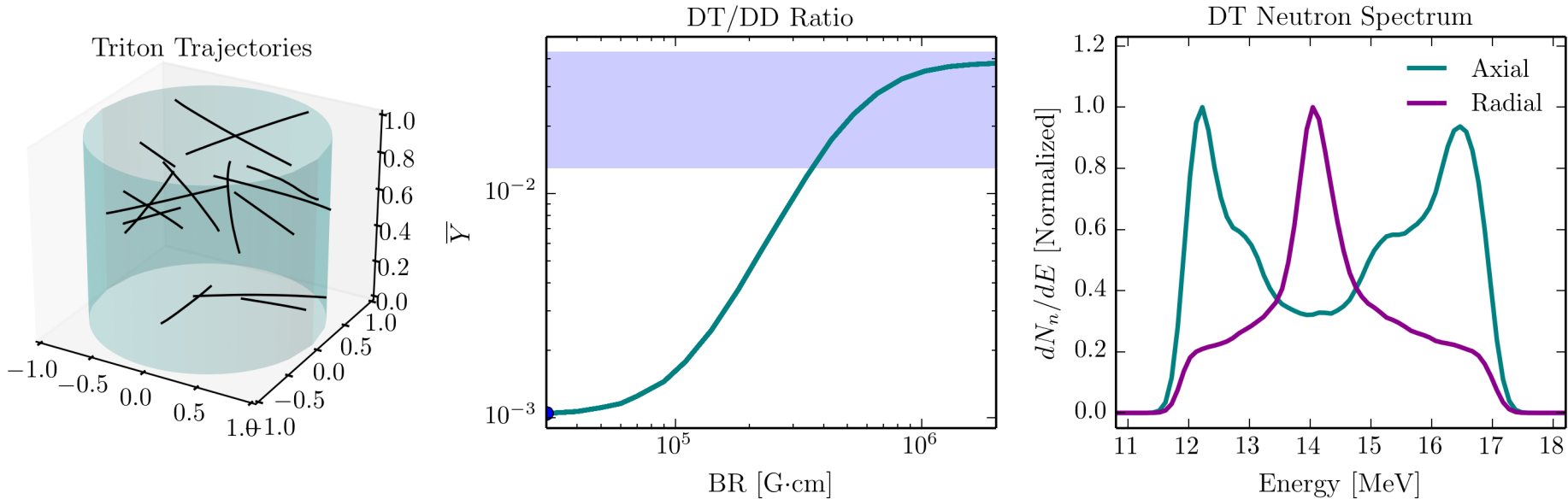


$$B \propto \rho$$



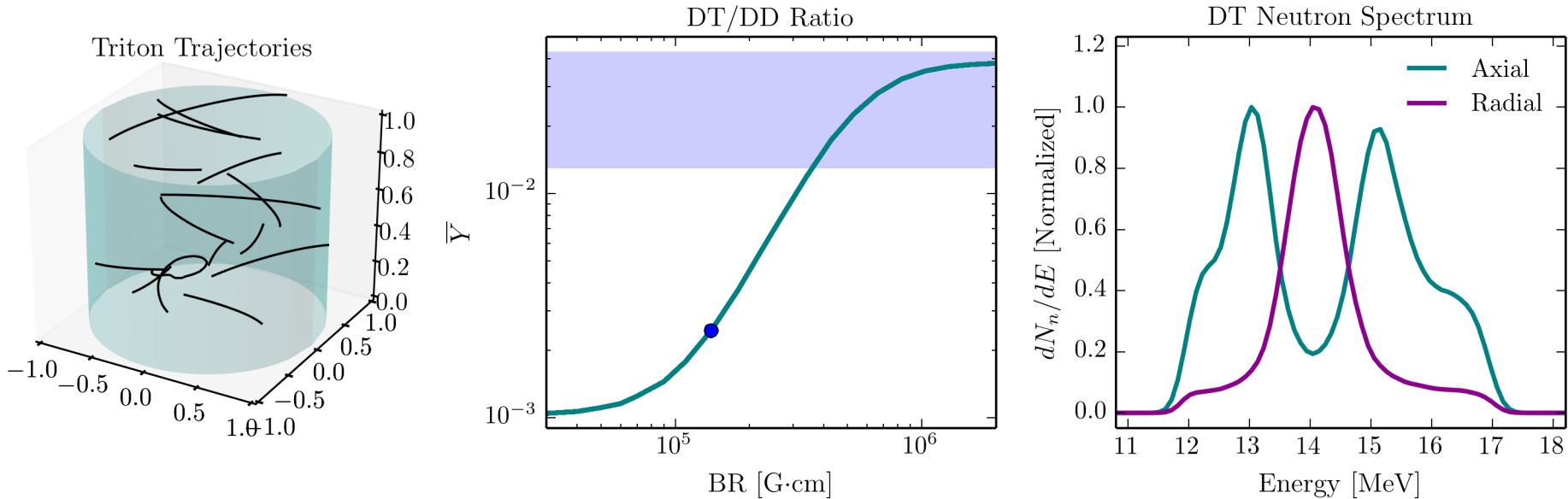
- [1] P.F. Schmit, P.F. Knapp *et al.* Phys. Rev. Lett. **113**, 155004 (2014)
 [2] P.F. Knapp, P.F. Schmit *et al.*, Phys. Plasmas **22**, 056312 (2015)
 [3] P.F. Schmit *et al.*, Phys. Plasmas **20**, 112705 (2013)
 [4] P.F. Knapp *et al.*, Phys. Plasmas **20**, 062701 (2013)

Magnetizing the tritons modifies their trajectories, imprinting on DT spectrum



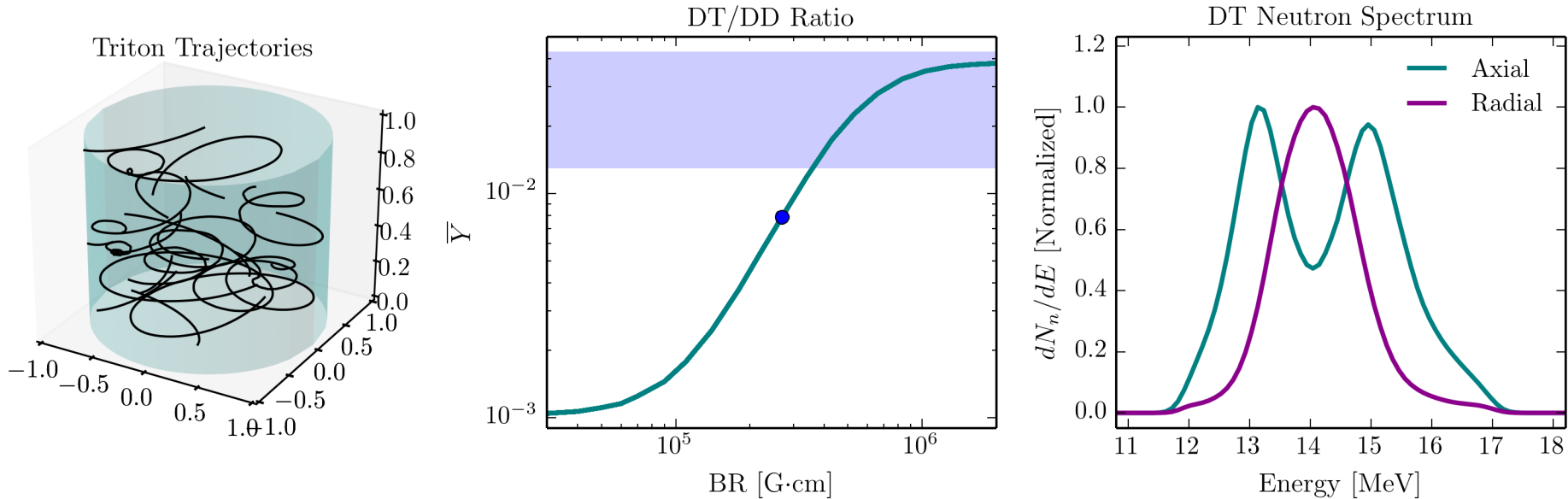
- Magnetization serves to:
 - Trap tritons
 - Direct them axially
 - Generate helical orbits
- Magnetization forces more and more tritons to see ρZ instead of ρR
 - $\rho Z = AR * \rho R, AR \gg 1$
 - broadens the velocity distribution of tritons that have a significant probability of reaction

Magnetizing the tritons modifies their trajectories, imprinting on DT spectrum



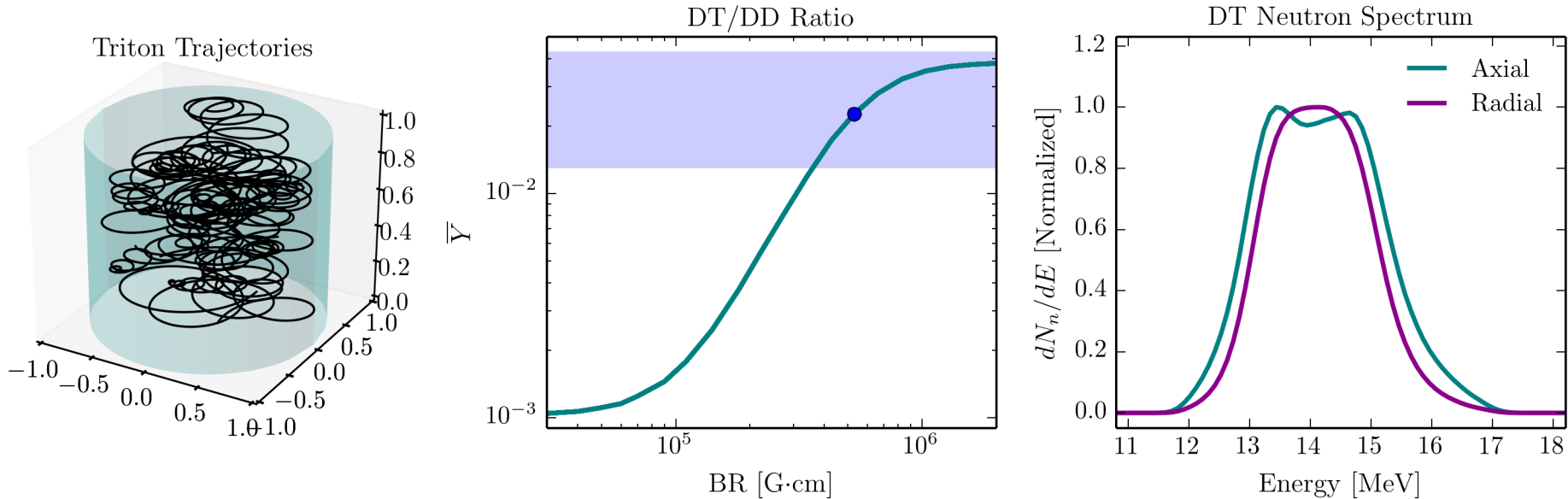
- Magnetization serves to:
 - Trap tritons
 - Direct them axially
 - Generate helical orbits
- Magnetization forces more and more tritons to see ρZ instead of ρR
 - $\rho Z = AR * \rho R, AR \gg 1$
 - broadens the velocity distribution of tritons that have a significant probability of reaction

Magnetizing the tritons modifies their trajectories, imprinting on DT spectrum



- Magnetization serves to:
 - Trap tritons
 - Direct them axially
 - Generate helical orbits
- Magnetization forces more and more tritons to see ρZ instead of ρR
 - $\rho Z = AR * \rho R, AR \gg 1$
 - broadens the velocity distribution of tritons that have a significant probability of reaction

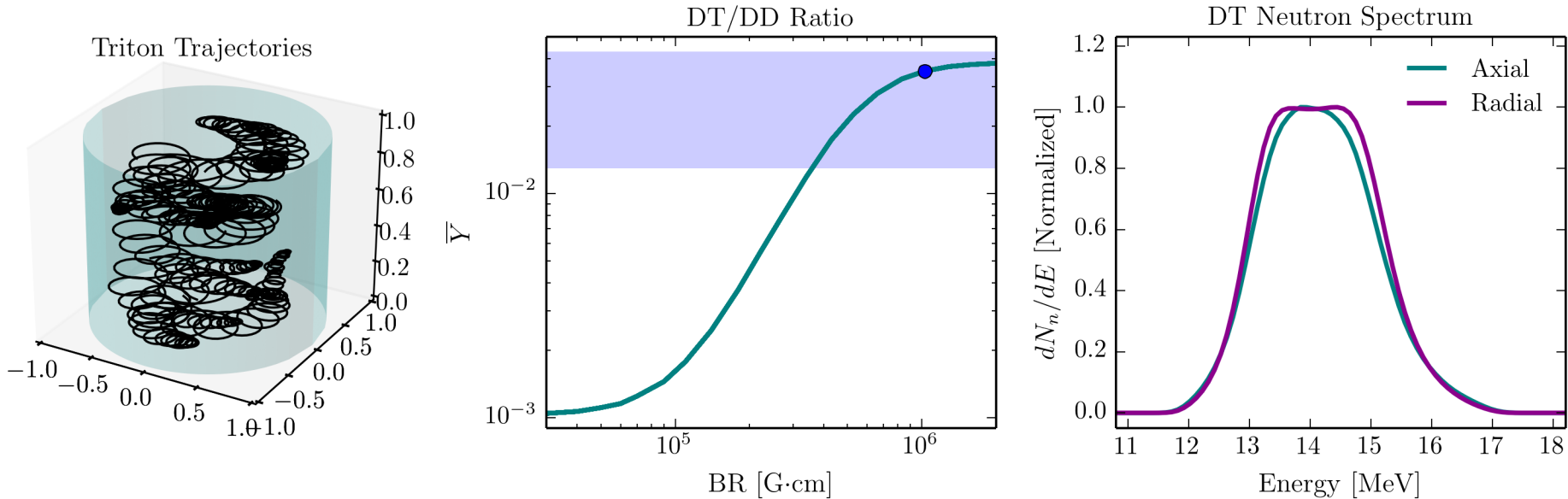
Magnetizing the tritons modifies their trajectories, imprinting on DT spectrum



- Magnetization serves to:
 - Trap tritons
 - Direct them axially
 - Generate helical orbits
- Magnetization forces more and more tritons to see ρZ instead of ρR
 - $\rho Z = AR * \rho R, AR \gg 1$
 - broadens the velocity distribution of tritons that have a significant probability of reaction

With sufficient BR , spectra tend to isotropize, plasma appears *infinite, homogeneous...* 18

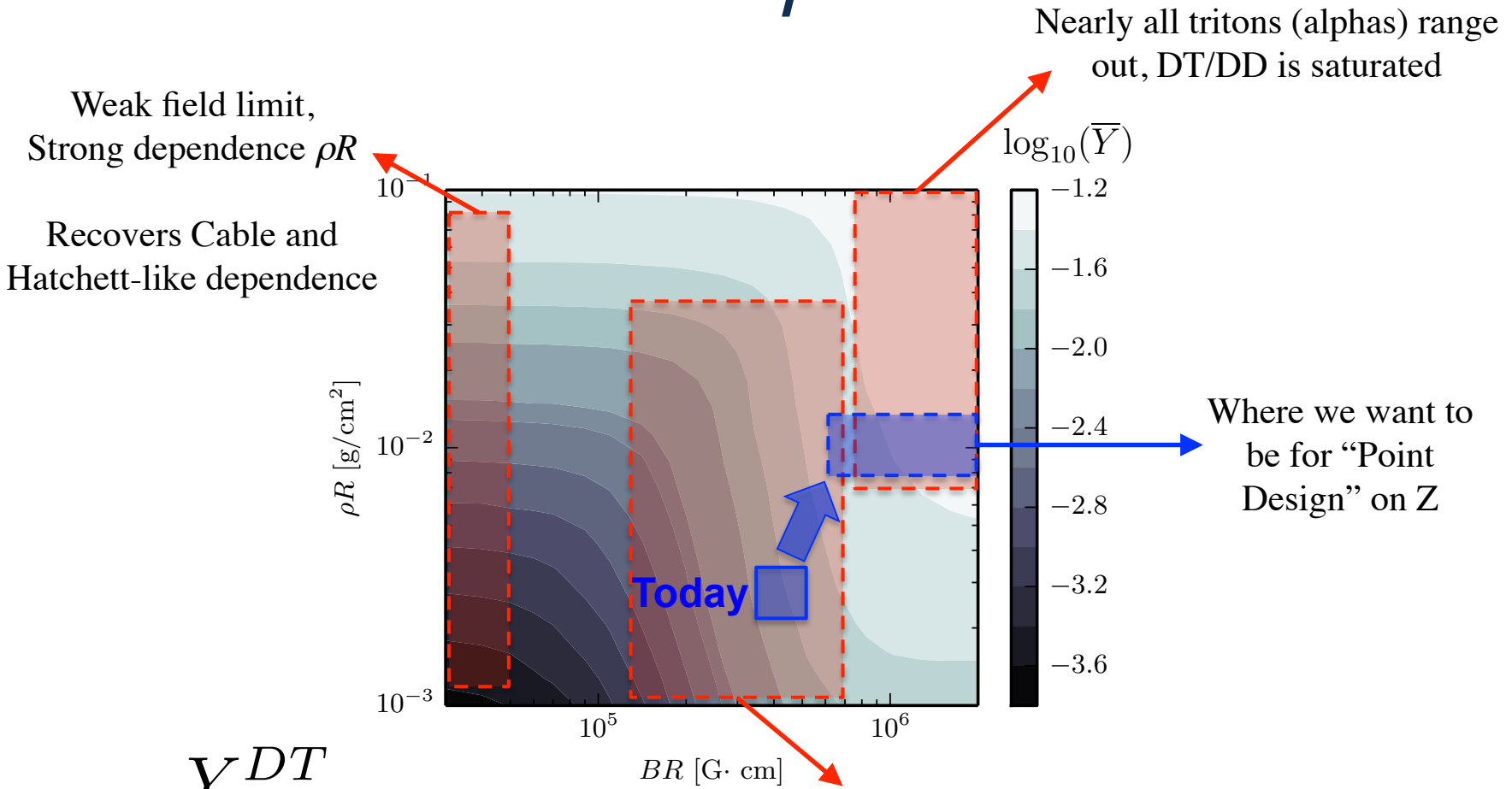
Magnetizing the tritons modifies their trajectories, imprinting on DT spectrum



- Magnetization serves to:
 - Trap tritons
 - Direct them axially
 - Execute helical orbits
- Magnetization forces more and more tritons to see ρZ instead of ρR
 - $\rho Z = AR * \rho R, AR \gg 1$
 - broadens the velocity distribution of tritons that have a significant probability of reaction

At large BR , finite length effects induce slight Doppler splitting in the radial view!

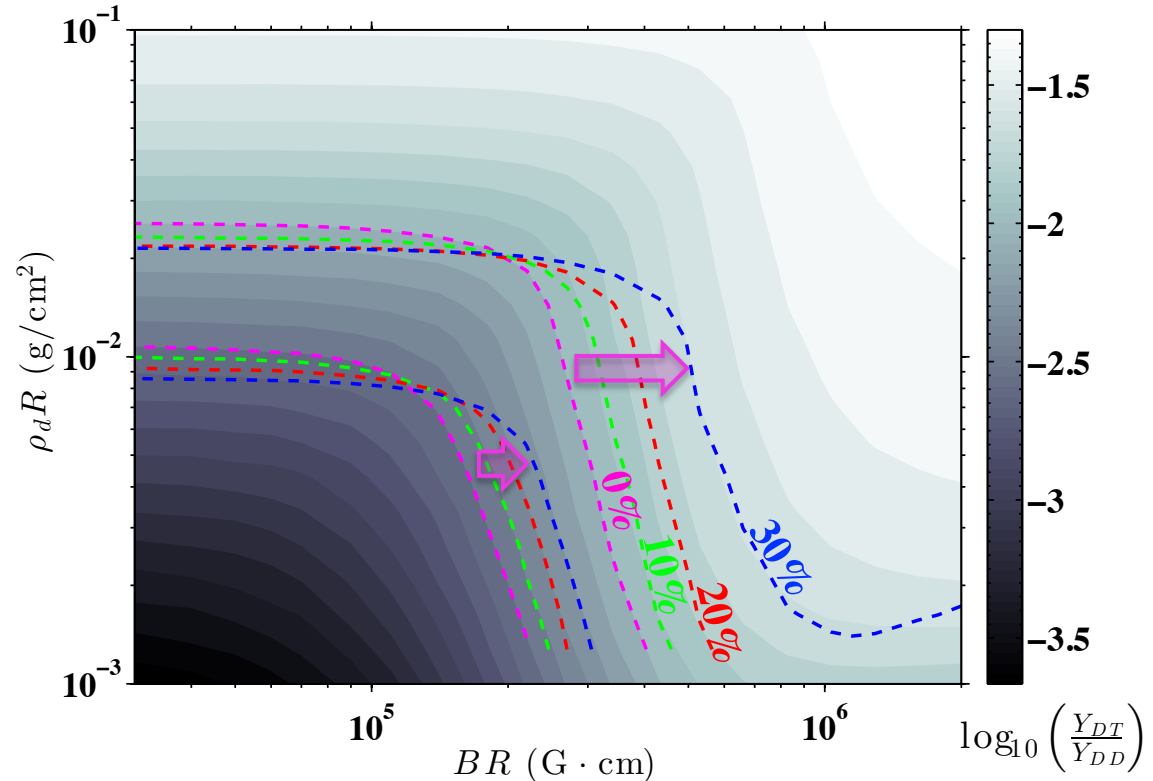
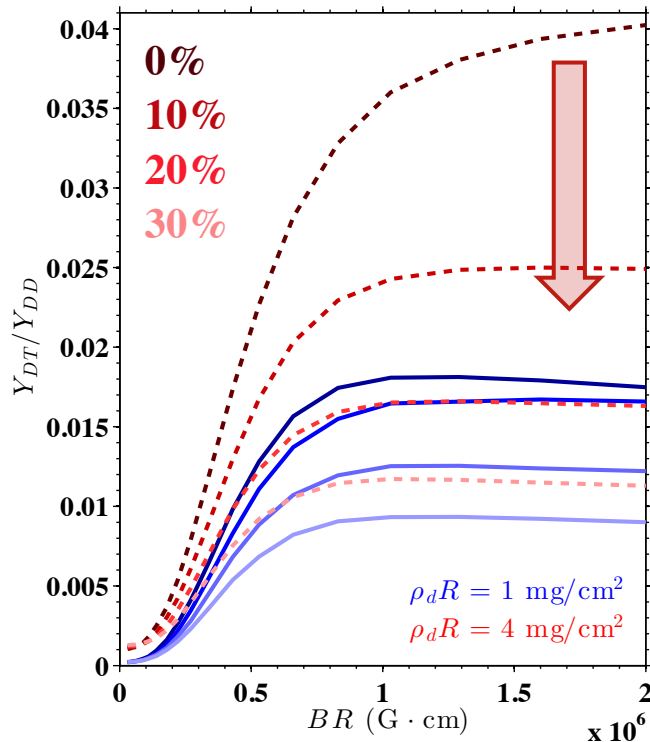
The DT/DD Ratio is a complicated function of BR and ρR



$$\bar{Y} = \frac{Y_{2n}^{DT}}{Y_{1n}^{DD}}$$

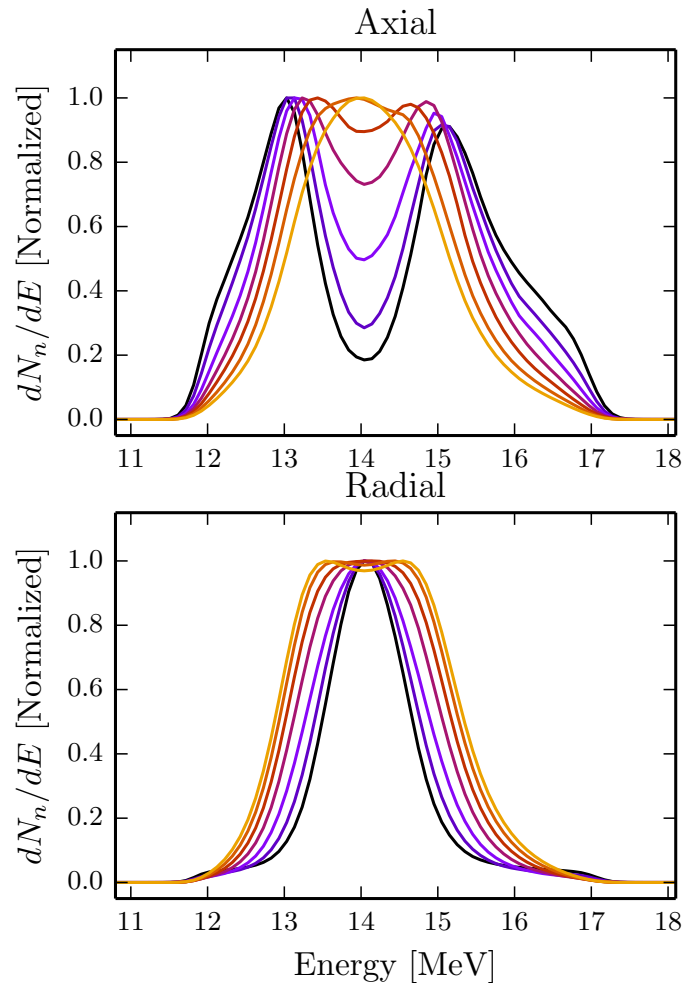
DT/DD is also affected by liner-fuel mix

Increasing Be mix fraction causes DT/DD to decrease, most noticeably at high BR
DT/DD provides a lower bound on inferred BR



- At low BR , mix acts like increasing ρR , adding electrons to enhance slowing
- At mid to high BR , mix decreases DT/DD by decreasing the path length of tritons
- Increases uncertainty in BR determined from DT/DD alone \rightarrow Mix diagnostic?

Secondary DT neutron Spectra are extremely sensitive to BR



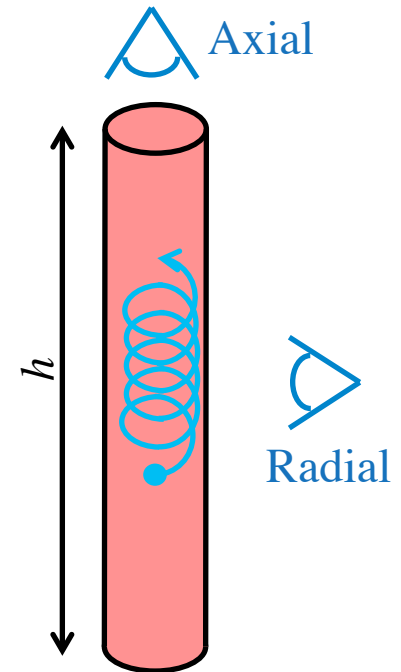
- In axial view, double-peak structure disappears as B isotropizes the initial trapped triton distribution
- Radial view broadens and begins to split

BR

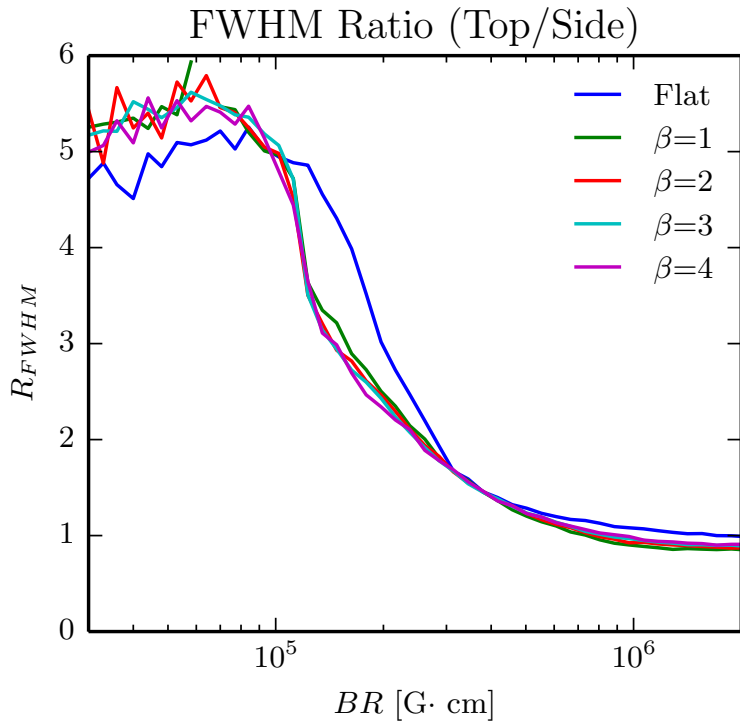
- 0.16 Mg·cm
- 0.2 Mg·cm
- 0.26 Mg·cm
- 0.33 Mg·cm
- 0.42 Mg·cm
- 0.54 Mg·cm
- 0.69 Mg·cm

$$BR \gtrsim 7 \times 10^5 G \cdot cm$$

Spectra isotropize and become insensitive to BR



FWHM ratio is sensitive to BR , insensitive to stopping physics

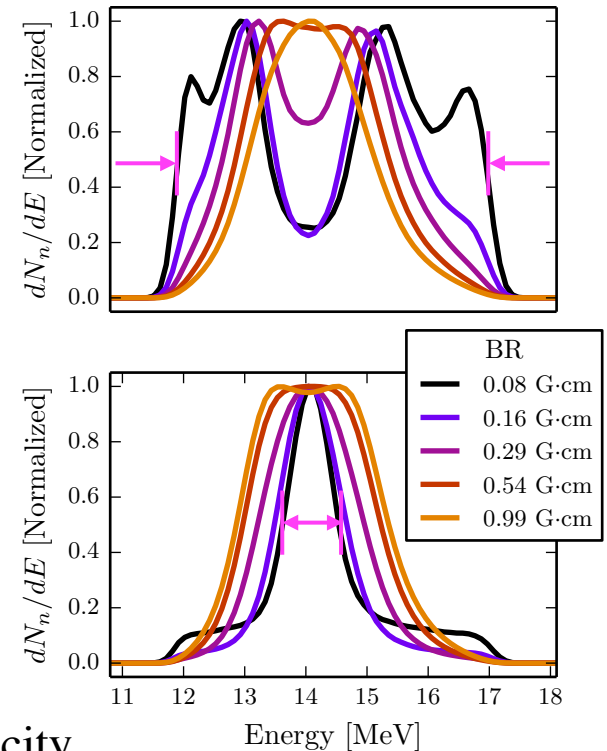


$$1 \text{ mg/cm}^2 \lesssim \rho R \lesssim 10 \text{ mg/cm}^2$$

$$10^5 \text{ G} \cdot \text{cm} \lesssim BR \lesssim 10^6 \text{ G} \cdot \text{cm}$$

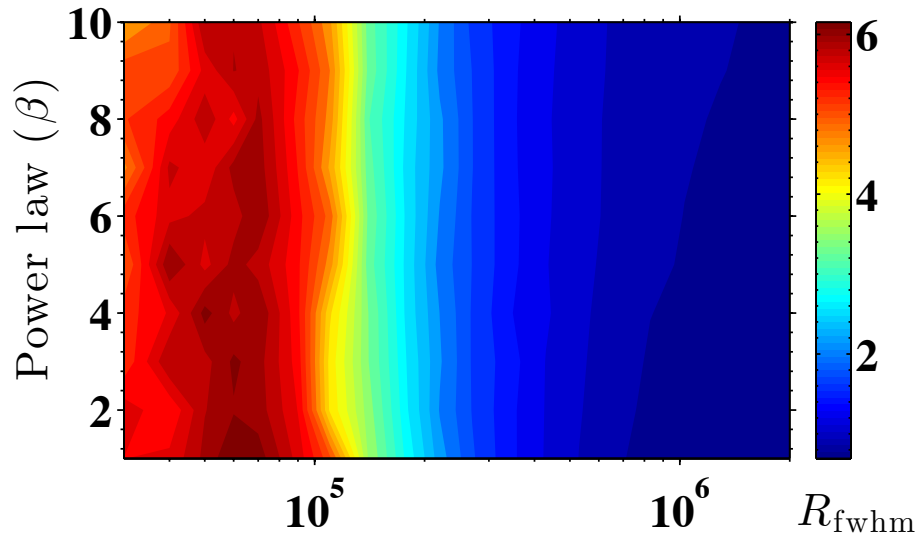
Considering the parameter space relevant to MagLIF and MIF in general

- Over a narrow (but interesting) range of BR , the FWHM ratio is basically insensitive to ρR , profile power law, etc.

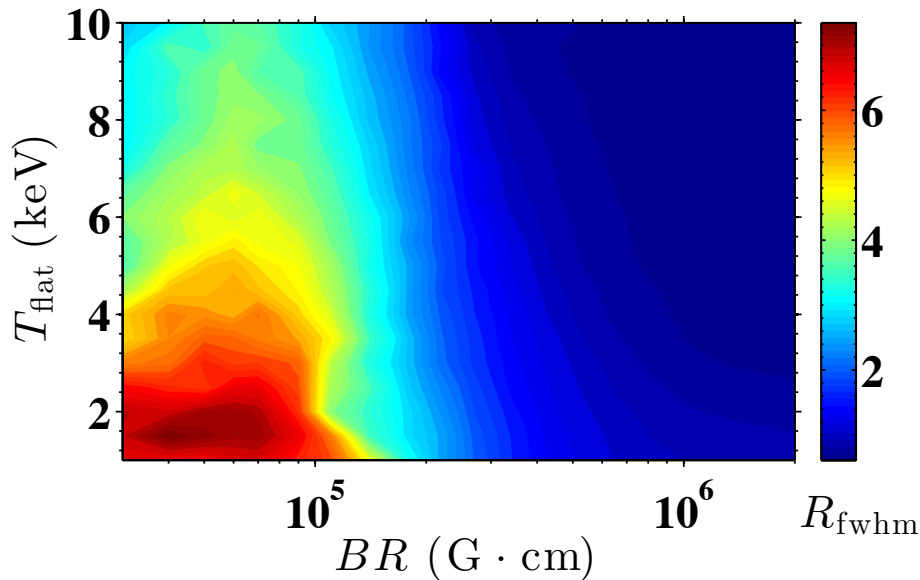


The “edges” of the spectrum depend largely on the *initial* velocity distribution of trapped tritons, not on the stopping physics

FWHM ratio is a robust metric, relatively insensitive to uncertainties in plasma conditions

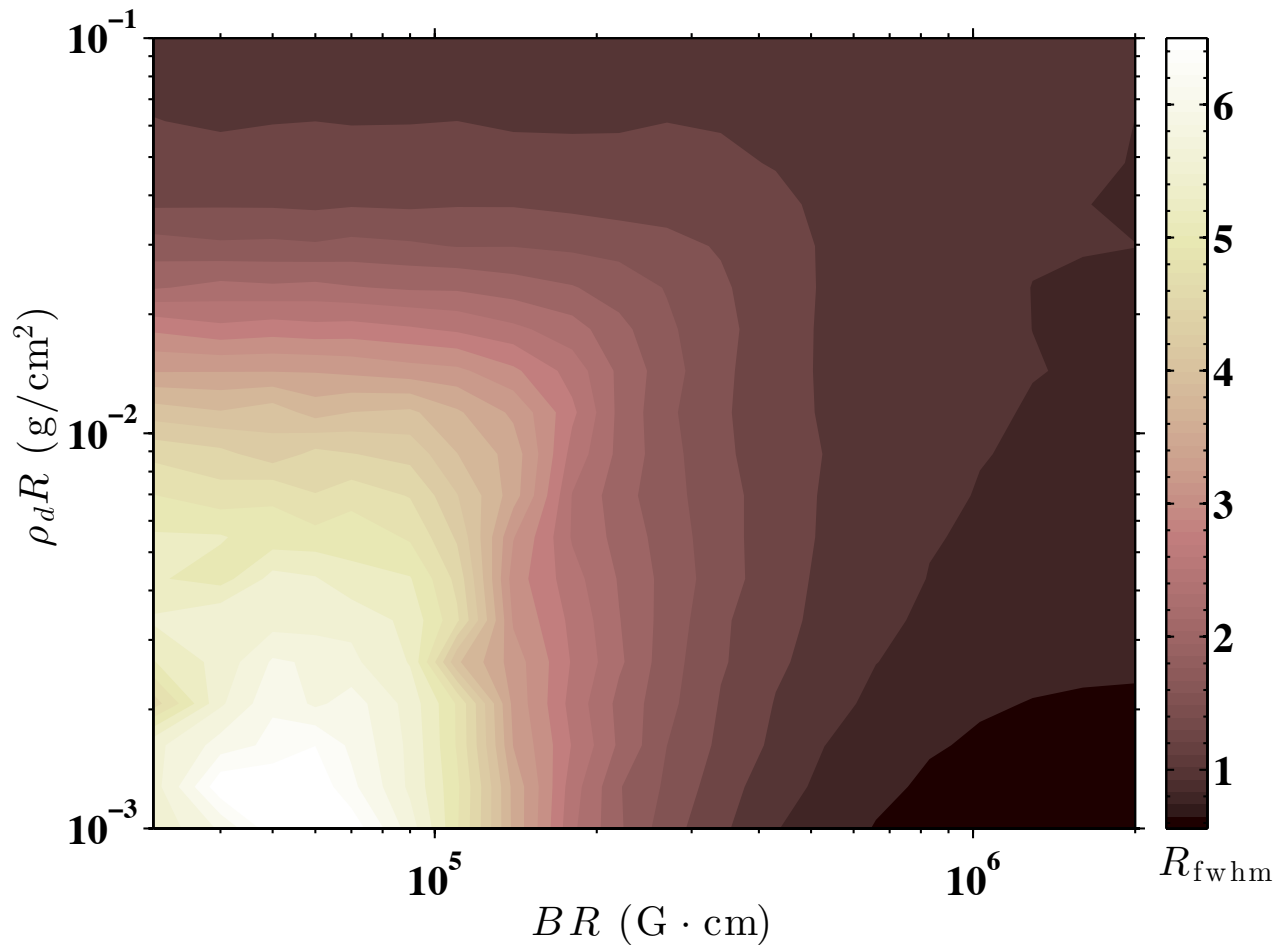


- Virtually insensitive to power-law index of the density/temperature profile, a poorly diagnosed quantity



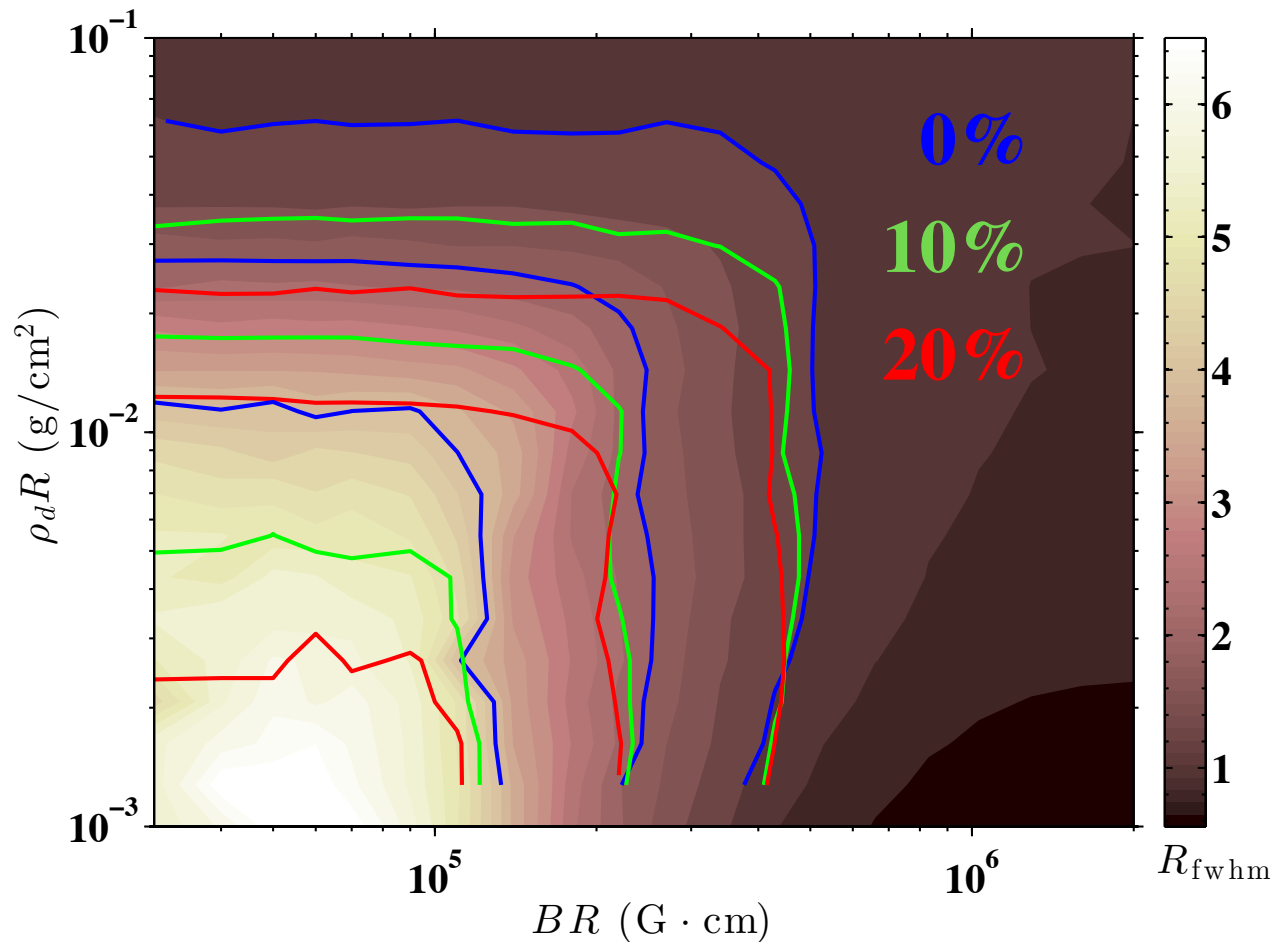
- Some T_e dependence, but one of the better-measured quantities

In region of interest, adding Be mix has a small impact on R_{fwhm}



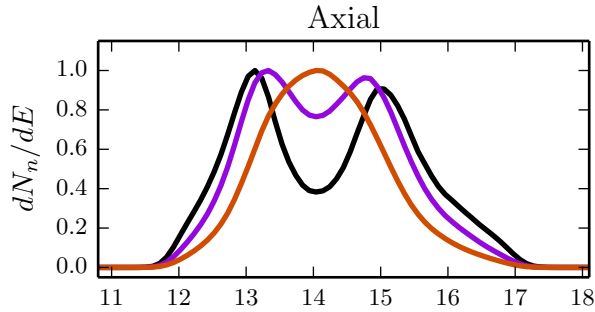
- ρR dependence is minimal for $BR < 6 \times 10^5$ Gcm
- For ρR up to ~ 10 mg/cm², R_{fwhm} is insensitive to ρR
- Adding a uniform concentration of Be on top of the fuel moves the R_{fwhm} contours slightly to the left
- The no-mix inference is an upper bound

In region of interest, adding Be mix has a small impact on R_{fwhm}



- ρR dependence is minimal for $BR < 6 \times 10^5$ Gcm
- For ρR up to ~ 10 mg/cm², R_{fwhm} is insensitive to ρR
- Adding a uniform concentration of Be on top of the fuel moves the R_{fwhm} contours slightly to the left
- The no-mix inference is an upper bound

DT Spectra are used in conjunction with measured DT/DD ratio to constrain the stagnation BR

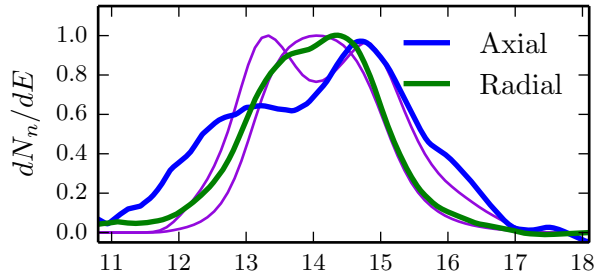


- $T_i \sim T_e = 3.1$ keV
- $\rho = 0.5$ g/cc
- $R = 50 - 100$ μm
- $\rho R = 2 - 5$ mg/cm²
- $\rho Z \sim 0.3$ g/cm²

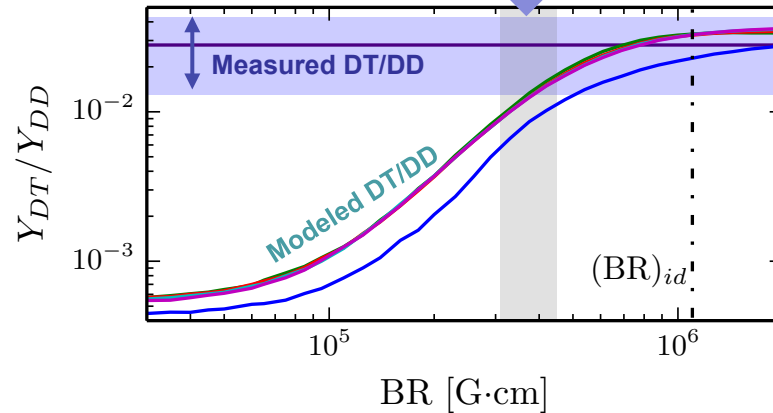
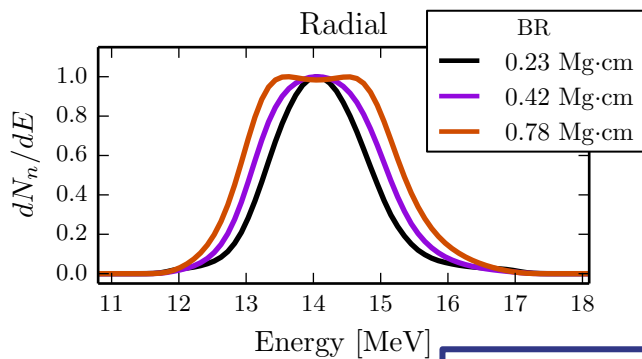
- Not a rigorous fit to the spectra
- Considering only the high energy half of the spectra
- In reasonable agreement with integrated 2D simulations^[*]

$$(B_z R)_{stag} = 5.3 \times 10^5 \text{ G} \cdot \text{cm}$$

$$F_t \approx 55\%$$



Inferred From Spectra



Axial nonuniformities and azimuthal field are the biggest missing features that can contribute to the modeled spectra

$$BR \approx 0.34(+0.14/-0.06) \text{ MG} \cdot \text{cm} \sim 14 \times (BR)_0$$

Experimentally inferred stagnation BR indicates we are trapping 1 MeV tritons and magnetizing electrons

- Modeling suggests we are depositing >35% of the triton energy
- Scales to >40% α deposition

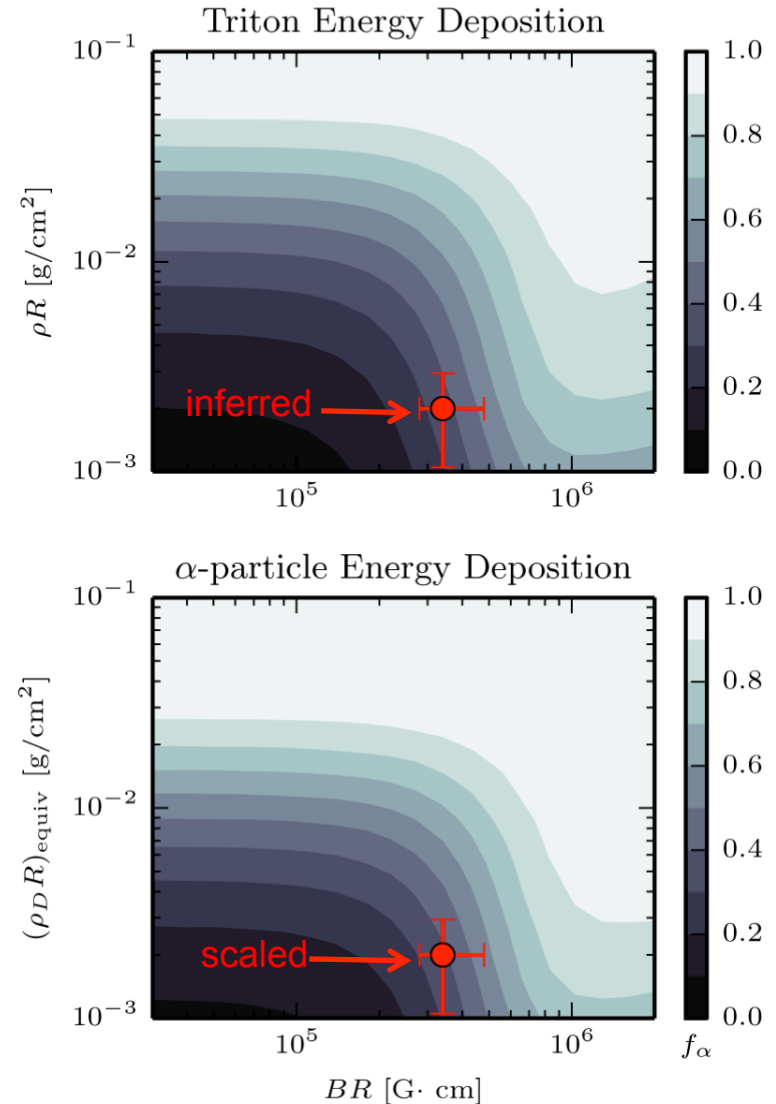
$$BR \sim 3.4 \times 10^5 G \cdot \text{cm} \rightarrow \frac{R}{r_\alpha} \sim 1 - 2$$

$$r_\alpha \approx 1.07 r_t$$

- Magnetizing fast tritons implies electrons are magnetized as well

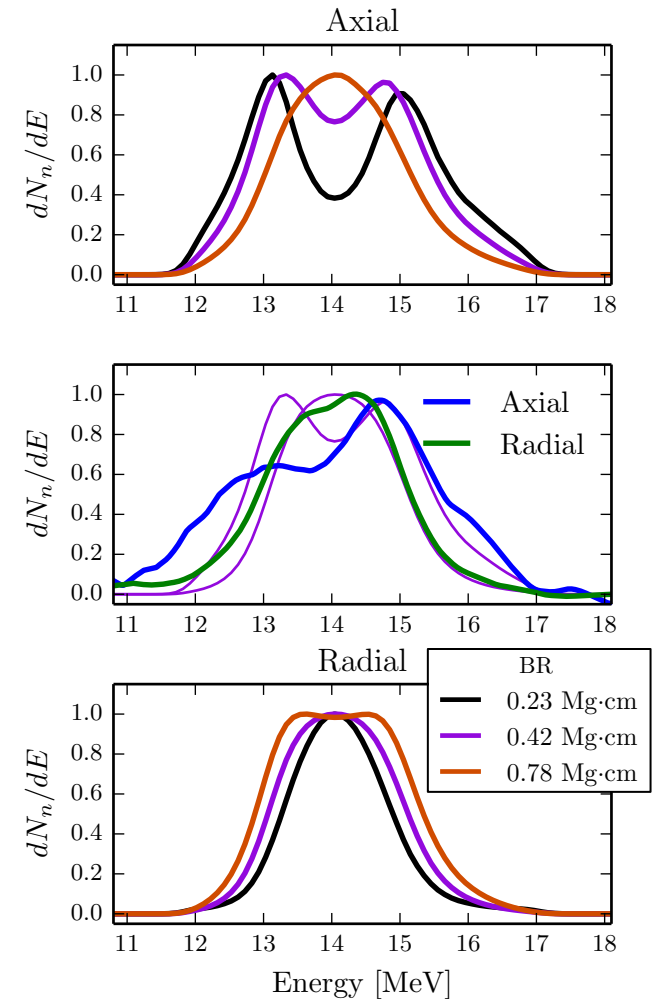
$$\omega_{ct} T_{te} \approx \omega_{ce} T_{ee}$$

MagLIF works! We were able to compress flux, preheat the plasma and keep it hot and magnetize the burn products!



Summary and Conclusion

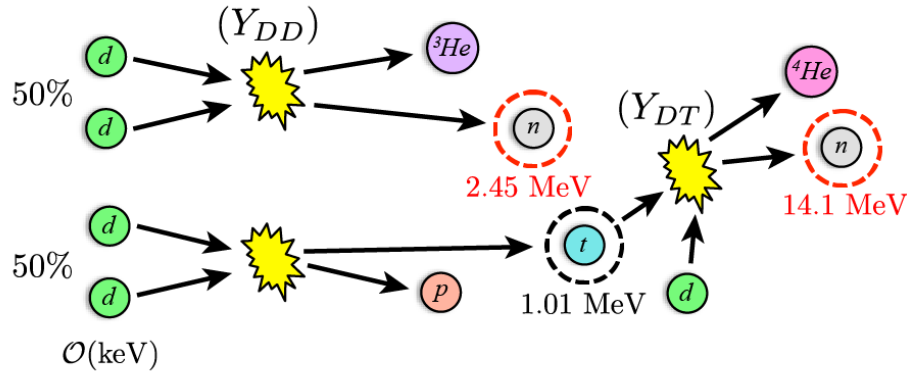
- We have made progress in understanding flux compression at stagnation
 - $\sim 400\times$ increase at stagnation in integrated experiments using neutron emission ($BR=3.4\times 10^5$ G \cdot cm)
- Significant challenges still exist
 - Would like to measure field strength throughout more of the implosion
 - Need to understand BR at stagnation with varying preheat and initial field strength (first “High-B” shots in December @ 20T)
- DT/DD ratio and DT neutron spectra together show that fusion tritons were confined at stagnation
- Inferred trapped fraction of charged burn products ($\sim 30\%$) shows we are nearing an ignition relevant regime



Backup slides

Modeling triton transport and reactions in magnetized plasmas

DD Fusion Reaction Branches



Probability of a triton reacting with a background deuteron:

$$P_i(\ell) = \int_0^\ell n_d(s) \sigma_{DT}(v_i(s)) ds \approx n_d \sigma_{DT} \ell$$

Unmagnetized

$$\frac{Y_{2n}^{DT}}{Y_{1n}^{DD}} \propto \rho R$$

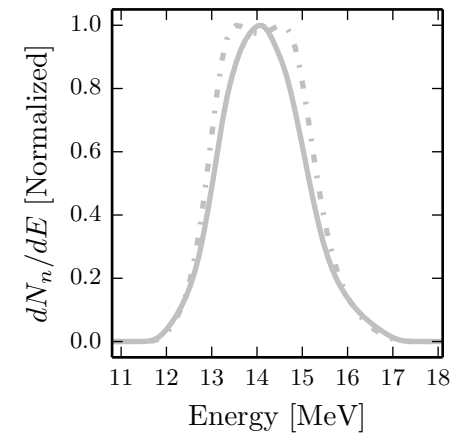
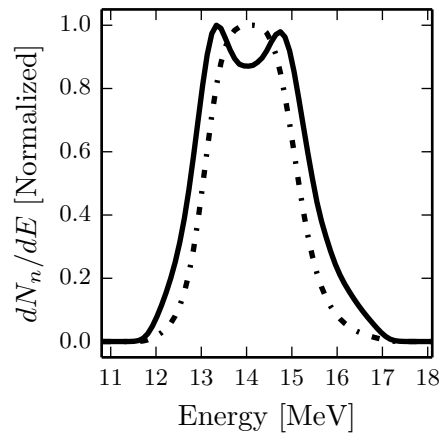
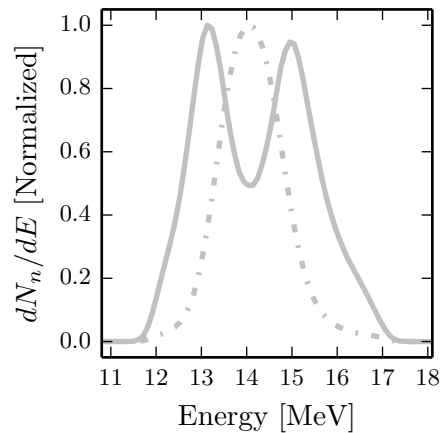
Magnetized

$$\frac{Y_{2n}^{DT}}{Y_{1n}^{DD}} \approx f(BR, \rho R)$$

- In limit of low ρR , increasing BR serves primarily to extend triton path length through fuel
- Magnetizing tritons effectively modifies the geometry they “see” as they travel through the fuel

Examining the triton “capture cone” gives insight into the spectral changes

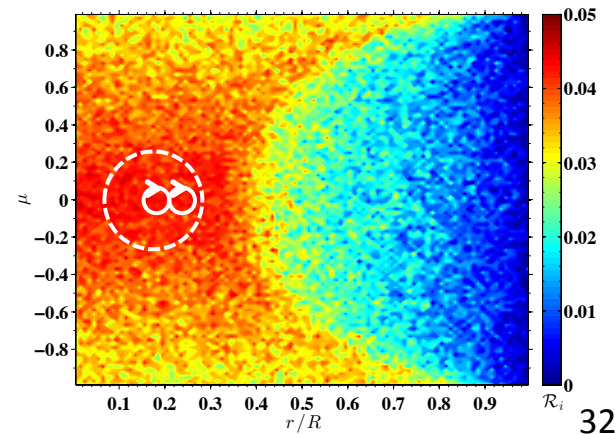
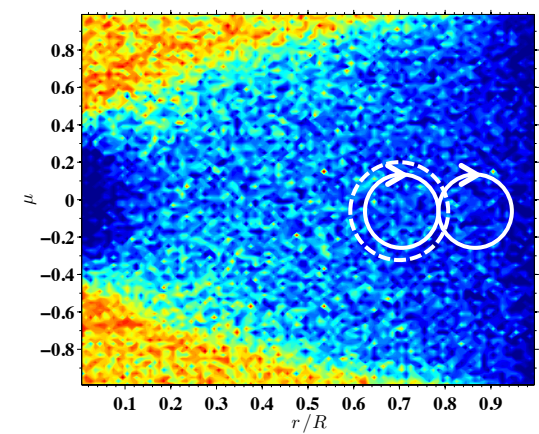
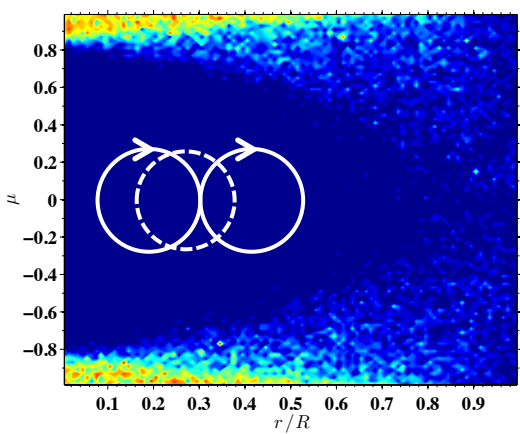
Increasing B field expands the triton capture cone (analogous to the loss cone in mirrors). These tritons sample more of the fuel volume as well as the triton velocity distribution, which tends to isotropize the spectrum



$BR = 2.5 \times 10^5 \text{ G} \cdot \text{cm}$

$BR = 4.5 \times 10^5 \text{ G} \cdot \text{cm}$

$BR = 7.5 \times 10^5 \text{ G} \cdot \text{cm}$



HYDRA (fluid) and LSP (particle) simulations are used to generate synthetic neutron spectra

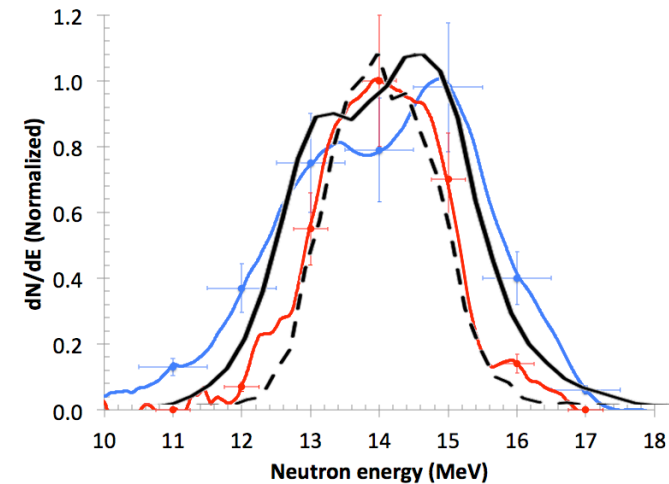
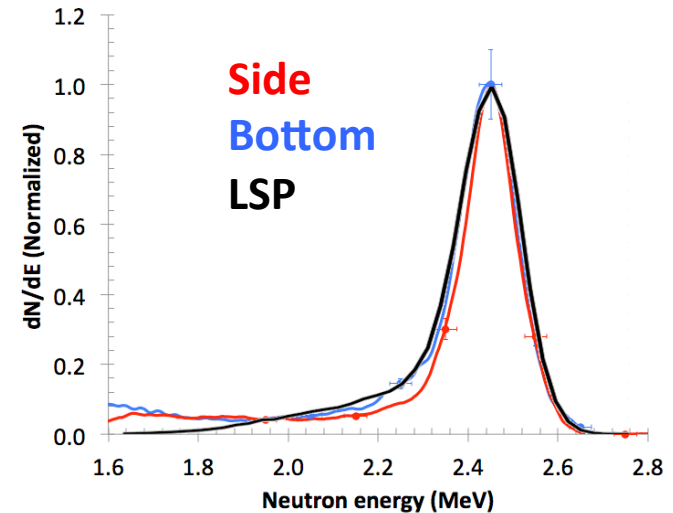
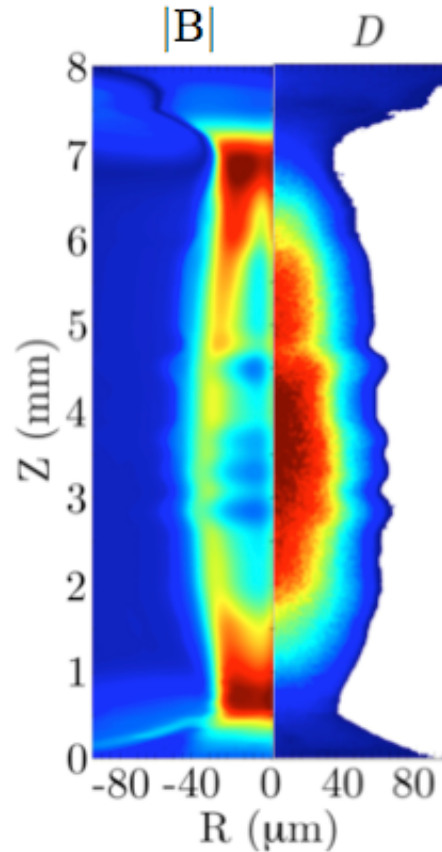
PIC simulations are initialized with HYDRA output (n , T , B) just before stagnation, and then run through burn.

ions are evolved kinetically

Binary scattering and fusion events

Synthetic neutron detectors are located to the side, top, and bottom

- Integrated stagnation BR is in close agreement with experimental inference
- Gross spectral features agree, left/right asymmetry of experiment reproduced well by integrated calculation




Understanding ρR , BR with DT/DD

- Triton range, λ , given by: $\lambda = \int_0^\infty v(t) dt = v_0 \int_0^\infty e^{-\nu_s t} dt = \frac{v_0}{\nu_s} \propto T_e^{3/2} / n_e$
- Reaction probability for “typical” fast triton in plasma of finite extent:
 - Probability per unit path length: $P_i[\mathbf{v}_i, \mathbf{x}] = n_d(\mathbf{x}) \int d\mathbf{v} (|\mathbf{v} - \mathbf{v}_i|/v_i) f_d(\mathbf{x}, \mathbf{v}) \sigma_{DT}(|\mathbf{v} - \mathbf{v}_i|)$
 $= n_d \langle \sigma v \rangle / v_i \equiv n_d \tilde{\sigma}[\mathbf{v}_i, \mathbf{x}]$

- Total probability before escape (small- ρR limit, homogeneous plasma)*:

$$\begin{aligned}
 P &= n_d \int_0^{\tau_{\text{esc}}} \tilde{\sigma}[v(t)] v(t) dt \\
 &\approx n_d v_0 \tau_{\text{esc}} \tilde{\sigma}_0 \\
 &\equiv n_d \langle r \rangle \tilde{\sigma}_0 \propto \rho \langle r \rangle
 \end{aligned}$$


 $v \approx v_0$

- Total probability in infinite homogeneous plasma:

$$\begin{aligned}
 P_\infty &= n_d \int_0^\infty \tilde{\sigma}[v(t)] v(t) dt \\
 &= n_d v_0 \int_0^\infty \tilde{\sigma}[v(t)] e^{-\nu_s t} dt \\
 &= \frac{n_d v_0}{\nu_s} \int_0^\infty \tilde{\sigma}[v(u)] e^{-u} du \\
 &= n_d \lambda \langle \tilde{\sigma} \rangle
 \end{aligned}$$

Density-independent, function of T_e only 

Assumes $P \ll 1$,
otherwise integrand
contains an additional
factor of $1 - P[\mathbf{x}(t)]$

- Trick with magnetized ICF plasma is noting that we are typically far from P_∞ , while $\langle r \rangle$ is a strong function of BR . Note that “trapped fraction” $\approx P_{\text{expt}} / P_\infty$